RESEARCH ARTICLE

Toxicity mechanism of silver nanoparticles to *Chlamydomonas reinhardtii*: photosynthesis, oxidative stress, membrane permeability, and ultrastructure analysis

Zhilin Zhao[1] · Limei Xu[1,2] · Yong Wang[2] · Bihan Li[2] · Wenming Zhang[3] · Xiaochen Li[1]

Abstract
Silver nanoparticles (Ag-NPs) are widely used in daily life and inevitably discharged into the aquatic environment, causing increasingly serious pollution. Research on the toxicity of Ag-NPs is still in infancy, little information is available on the relationships between oxidative stress and antioxidant, as well as damaging degrees of Ag-NPs to cellular structural components of *Chlamydomonas reinhardtii* (*C. reinhardtiii*). In the present study, we revealed the toxicity mechanism of *C. reinhardtii* under Ag-NPs stress using flow cytometry (FCM), metabolic methods, and transmission electron microscopy. The results showed that the chloroplasts were damaged and the synthesis of photosynthetic pigments was inhibited under Ag-NPs stress, which inhibited the growth of *C. reinhardtii*. Meanwhile, Ag-NPs also caused *C. reinhardtii* to produce excessive reactive oxygen species (ROS), increased malondialdehyde content and changed the permeability of cell membrane, resulting in the acceleration of internalization of Ag-NPs. The decrease of cell size and intracellular chlorophyll autofluorescence was observed with FCM. To deal with the induced excessive ROS that could lead to lethal and irreversible structure damage, *C. reinhardtii* activated antioxidant enzymes including superoxide dismutase and peroxidase. This study provides new information for better understanding the potential toxicity risks of Ag-NPs in the aquatic environment.

Keywords Silver nanoparticles · *Chlamydomonas reinhardtii* · Oxidative stress · Toxicity mechanism · Ultrastructure

Introduction

The rapid development of nanotechnology has a significant impact on the economy, society, and the environment (Ji et al. 2011). Nanomaterials have been used widely in industrial sectors, medicine, and environmental areas because of their small size, distinctive structure, and surface properties (Froehlich 2012; Kachynski et al. 2008; Wei et al. 2008). However, while bringing convenience to human, nanomaterials are inevitably released to the environment (Manier et al. 2013; Wiesner et al. 2006). In fact, the interactions between nanoparticles and aquatic organisms have been clearly identified (Oukarroum 2014), and therefore, human are increasingly concerning about the impact and potential risks of nanoparticles to natural environment (Li et al. 2011; Wiesner et al. 2006).

Silver nanoparticles (Ag-NPs) are noted for excellent broad-spectrum of antimicrobial properties and their special conductivity and photochemical properties. They have been extensively used in antimicrobial agent, electronic devices, and wastewater treatment (Echavarri-Bravo et al. 2017; Tran et al. 2013; Zhang et al. 2016). Previous studies found that Ag-NPs enter the aquatic environment through wastewater discharges as well as absorbing on soil particles that were transported by surface run-off (Dewez et al. 2018). Hoque et al. (2012) found that the concentration of Ag-NPs in the wastewater was 1.9 μg/L from a Canadian wastewater treatment plant; and Boxall et al. (2007) predicted that Ag-NPs in surface water could reach above 0.1 μg/L. Therefore, the potential toxicity of Ag-NPs to various organisms in the aquatic environment has received widespread attention.

Zhilin Zhao and Limei Xu contributed equally to this work.

Responsible Editor: Ludek Blaha

✉ Xiaochen Li
lixiaochen02@163.com

[1] Water Conservancy and Civil Engineering College, Shandong Agricultural University, Tai'an 271018, Shandong, China

[2] State Key Laboratory of Crop Biology, College of Life Sciences, Shandong Agricultural University, Tai'an 271018, Shandong, China

[3] Department of Civil and Environmental Engineering, University of Alberta, Edmonton, AB T6G 1H9, Canada

Previous studies have indicated that Ag-NPs are toxic to algae, bacteria, zooplankton, and fish (Bruneau et al. 2016; Choi et al. 2018; Cui et al. 2017; Hazani et al. 2013). For example, Ag-NPs deteriorated the water splitting system of photosystem II (PSII) and inactivated the PSII reaction centers, which led to inhibition of photosynthetic process and growth of *Lemna gibba* (Dewez et al. 2018). Ag-NPs also caused oxidative stress in *Escherichia coli K-12*, increased the activity of antioxidant enzymes, and showed obvious damage to cell membranes (Choi et al. 2018). After Ag-NPs exposure, Japanese medaka at early-life stages showed morphological abnormalities (edema, spinal abnormalities, finfold abnormalities, heart malformations, and eye defects) and growth retardation (Wu et al. 2010). Therefore, Ag-NPs have posed significant threats to aquatic ecosystems.

Microalgae are important primary producers that provide biological energy and oxygen to organisms of other trophic levels, and play very important roles in maintaining the material balance and energy cycle of aquatic ecosystems (Yu et al. 2018). Microalgae are also used as a model organism to assess the potential toxicity of a harmful substance to aquatic ecosystems (Jagadeesh et al. 2015; Wang et al. 2011). As a specie of microalgae, *Chlamydomonas reinhardtii* (*C. reinhardtii*) is a biflagellate photosynthetic unicellular organism that is easy to cultivate and highly sensitive to environmental pollution (Nowicka et al. 2016; Pröschold et al. 2005), and thus can be used as an environmental monitor. *C. reinhardtii* is widespread in freshwater and it inevitably interacts with Ag-NPs in the aquatic environment. Previous studies have also compared the toxicity of Ag-NPs with silver ions (Ag^+). Toxicity of Ag^+ against algae has been widely studied in previous works, including the inhibition of growth and photosynthesis (Hiriart-Baer et al. 2006; Lee et al. 2005; Ke et al. 2018), the production of excessive reactive oxygen species (ROS) (Sendra et al. 2017; Lu et al. 2020), and the increasing of cell membrane permeability (Lu et al. 2020). Previous researchers also found that toxicity of Ag^+ to organisms was greatly higher than that of Ag-NPs, such as *Escherichia coli K-12* strain (Choi et al. 2018), *Daphnia magna* (Hu et al. 2018), and *Dunaliella salina* (Johari et al. 2018). In fact, previous related researches suggested that Ag^+ and Ag-NPs could both posed extensively toxic effects to organisms; however, the toxic mechanisms might be fall in different pathways. For instance, results of Ke et al. (2018) indicated that both Ag-NPs and Ag^+ can inhibit the growth and photosynthesis of *Arabidopsis thaliana*, while Ag-NPs can also regulate shikimate-phenylpropanoid biosynthesis, and tryptophan and galactose metabolisms. Research on the toxicity of Ag-NPs is still in infancy, little information is available on the relationships between oxidative stress and antioxidant, as well as damaging degrees of Ag-NPs to cellular structural components of *C. reinhardtii*. Therefore, it is of great interest to comprehensively study the effects of Ag-NPs on these aspects of

C. reinhardtii and obtain the toxicity mechanism, which are necessary to fully reveal the aquatic environmental risks of Ag-NPs.

In this study, we investigated the effects of Ag-NPs on *C. reinhardtiii* growth (biomass, cell size); photosynthesis (photosynthetic pigment content, chloroplast damage); oxidative stress (ROS, superoxide dismutase (SOD) activity, and peroxidase (POD) activity); cell membrane permeability (malondialdehyde (MDA) content, number of non-viable cells); and cell ultrastructure. Based on the analysis above, the toxicity mechanism of Ag-NPs to *C. reinhardtiii* was discussed. The results of this study contribute to better understanding of the toxicity risks of Ag-NPs in aquatic environment.

Materials and methods

Culture of *C. reinhardtii*

C. reinhardtii (FACHB-265) was obtained from the Freshwater Algae Culture Collection at the Institute of Hydrobiology (FACHB), Wuhan, China. *C. reinhardtii* was inoculated in Selenite Enrichment (SE) medium (Table S1) and cultured in a light incubator at 25 ± 1 °C, under light intensity of 2000 ± 50 lx with 12 h (light): 12 h (dark) cycle. The cultures were shaken 3–5 times daily. The logarithmic algal solution was diluted with SE medium to obtain an initial cell density of approximately 1×10^6 cells/mL for all experiments.

Toxicological studies

Ag-NPs (60–120 nm in diameter; 99.5% purity) were from Aladdin Reagent Co., Shanghai, China. The chemical composition of Ag-NPs was analyzed by inductively coupled plasma mass spectrometry (7700 ICPMS, Agilent Technologies Inc., America). The morphology of the Ag-NPs was characterized with a scanning electron microscope (SEM) (Sigma 300, Japan) with scanning voltage of 8 kV. To achieve stock suspensions of 500 mg/L, 0.25 g Ag-NPs was uniformly dispersed in 500 mL SE medium with 2 h ultrasonic treatment (200 W, 40 KHz). Different volumes of stock solution were added to the original algal solution for exposure tests. The concentration of Ag-NPs used in acute tests was 0, 1, 5, 10, 30, and 50 mg/L, respectively. Particle size distribution and zeta potential of Ag-NPs in the culture media were performed by using dynamic light scattering (DLS) analysis with a Laser Nanometer Particle Size Analyzer (Zetasizer-Nano-ZS, Malvern Instruments, UK). The Ag^+ content was determined by atomic absorption spectrophotometry (TAS-990, Beijing Purkinje General Instrument Co., Ltd., China). After 24, 48, 72, 96, and 120 h exposure, *C. reinhardtii* cells were counted by a hemocytometer under a light microscope (YS100, Shanghai Lichi Measuring Instrument Co., Ltd., China).

Inhibitory rate of growth was determined by the following formula:

$$(IR)\% = (1 - N/N_0) \times 100\%$$

where N is the cell density (cells/mL) in the Ag-NPs treated culture, and N_0 is the cell density (cells/mL) in the control culture. The medium effective concentration (EC_{50}) of cell growth inhibition was calculated by SPSS software.

Chlorophyll pigments determination

Twenty milliliters of algal cell suspension was filtered through a 0.45-μm membrane. The membrane was then cut into strips and suspended in 5 mL of 80% acetone. The extracted algal solution was crushed in an ice bath environment (0–4 °C) for 6 min and then centrifuged at 5000 r/min for 10 min. Acetone was used as a blank, and absorbance values of the supernatant at 663 nm, 646 nm, and 470 nm were measured with a UV-visible spectrophotometer (UV-245, Shimadzu Enterprise Management Co., Ltd., China). The chlorophyll pigments were calculated by using the following formula:

$$C_a = 12.21A_{663} - 2.81A_{646}$$

$$C_b = 20.13A_{646} - 5.03A_{663}$$

$$C_{x+c} = \frac{1000A_{470} - 3.27 \times C_a - 104 \times C_b}{229}$$

$$C_T = C_a + C_b$$

where C_a, C_b, C_{x+c} and C_T are the concentration of chlorophyll a, chlorophyll b, carotenoids, and total chlorophylls, respectively.

Flow cytometry analysis

Cell size, intracellular chlorophyll autofluorescence, cell viability, and oxidative stress were measured by flow cytometry (BD LSR Fortessa 4, Becton, Dickinson and Company, USA). Forward-scattered light (FSC), side-scattered light (SSC), and red autofluorescence (FL4 channel: 660–700 nm) indicate cell size, cell complexity, and chlorophyll, respectively. Propidium iodide (PI) is a fluorescent dye that binds to a nucleic acid macromolecular substance and produces orange fluorescence under blue light excitation. PI only passes through damaged membrane. In this study, fluorescence of cells stained with PI was measured to determine the cell viability and membrane integrity (Suman et al. 2015). The permeable dye indicator 2′,7′-dichlorodihydrofluorescein diacetate (H$_2$DCFDA, green fluorescence) is a non-polar compound that can be used to determine the production of intracellular ROS such as H_2O_2, hydroxyl radical (•OH) and superoxide anion radical (•O_2^-) (Oukarroum 2014).

Algal cell suspension (1 mL) was stained with 60 μM PI or 80 μM H$_2$DCFDA and incubated for 30 min in the dark. The cells were harvested by repeating centrifugation twice (at 3500 r/min for 10 min), washed with 1 mL precooled phosphate buffer solution (PBS, pH = 7), and then resuspended in 1 mL PBS. The mixture was then filtered through a 200-mesh screen. Experiment data was collected from 10,000 cells. The cell viability and production of intracellular ROS were measured by using orange fluorescence (FL3 channel: 533/30 nm) and green fluorescence (FL1 channel: 605–635 nm). Positive controls for cell viability and ROS production were 100% heat-damaged cells at 99 °C for 30 min and 0.1 mM H$_2$O$_2$-treated cells, respectively. Negative controls were cells without Ag-NPs treatment.

POD, SOD, and MDA assays

The POD and SOD activities and stress indicator MDA were determined with different assay kits (POD: A084-3-1; SOD: A001-1-1; MDA: A003-1-2; Nanjing Jiancheng Bioengineering Institute, China). Forty milliliters of algal cell suspension was centrifuged at 3500 r/min for 5 min. The collected algal cells were washed twice and re-susupended with different precooled buffers (POD: 0.05 mol/L PBS, pH = 5.5; SOD: 0.05 mol/L PBS, pH = 7.8; MDA: 5% trichloroacetic acid). The cell suspensions were crushed in ice bath for 3 min by ultrasonic cell crusher (Scientz-IID, Ningbo Xinzhi Biotechnology Co., Ltd., China) and then centrifuged at 3500 r/min for 20 min. The supernatants were transferred to new microtubes for POD, SOD, and MDA analyses according to the manufacturer's instructions.

TEM observation of algal cells

The effects of Ag-NPs on the ultrastructure of *C. reinhardtii* were observed with a biological transmission electron microscope (TEM, H-7650, Hitachi, Japan). Fifty milliliters control (in logarithmic growth phase) and 72-h Ag-NPs-treated (1, 10, and 50 mg/L of Ag-NPs) algal cell suspensions were centrifuged and the supernatant was discarded. Then, these samples were treated by double fixation, washing, dehydration, infiltration, and embedding according to the method of (Perreault et al. 2012). The treated samples were cut into 70–90 nm slices, stained with uranyl acetate (saturated solution in 50% ethanol) for 10 min and lead citrate solution for 10 min, and analyzed by the TEM. Each sample was analyzed for multiple fields of view at different magnifications.
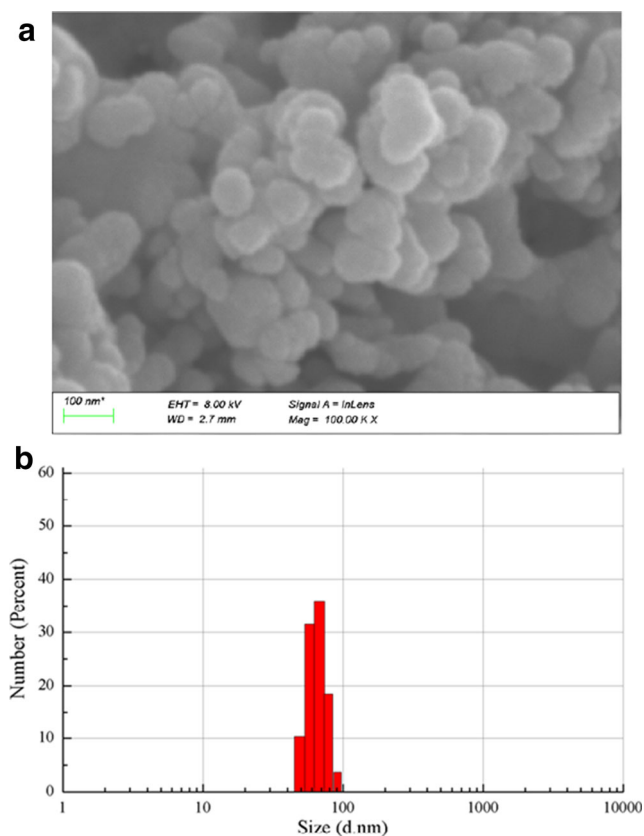
Statistical analysis

All treatments were conducted in triplicates. Mean and standard deviation were calculated for each treatment. Significant differences between means were determined by analysis of

one-way ANOVA (IBM SPSS, Statistics 19 program). P values < 0.05 were considered to be significantly different. All flow cytometry (FCM) data were analyzed by using FlowJo V10 software. Origin 9 was used to plot graphs.

Results

Characterization of Ag-NPs

The composition analysis of the Ag-NPs used in this study was shown in Table S2. It can be observed from Table S2 that the used Ag-NPs are composed of 99.9% simple substance of silver. SEM image confirmed that the morphology of Ag-NPs was mostly spherical particles with a diameter range of 60–120 nm (Fig. 1a). The particle size of Ag-NPs in SE medium analyzed by DLS showed a normal distribution with a median diameter of 68.1 nm (Fig. 1b). The zeta potential of the Ag-NPs suspension was -18.8 mV, indicating that Ag-NPs surface was negatively charged and the suspension was relatively stable. About 0.45% of the Ag-NPs were present as Ag^+, indicating that the amount of Ag^+ released was very little.
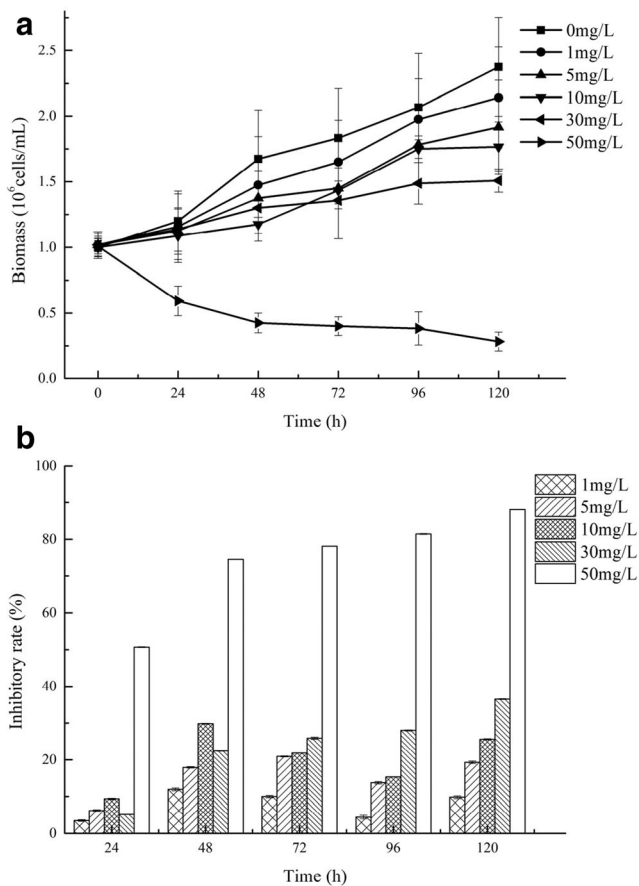
Effects of Ag-NPs on the growth of C. reinhardtii

The effects of 0–50 mg/L Ag-NPs after exposures of 0–120 h on the biomass of C.reinhardtii are shown in Fig. 2a. The biomass of C. reinhardtii still increased with 1–30 mg/L Ag-NPs, while it declined dramatically when Ag-NPs concentration reached 50 mg/L. The inhibitory effect became more and more obvious with the increase of exposure concentrations and time as shown in Fig. 2a and b. At 96 h, the inhibition rates of 1, 5, 10, 30, and 50 mg/L Ag-NPs were $4.45 \pm 0.50\%$, $13.74 \pm 0.30\%$, $15.34 \pm 0.07\%$, $28.01 \pm 0.16\%$, and $81.47 \pm 0.13\%$, respectively. The maximum inhibition rate ($88.08 \pm 0.07\%$) occurred at 50 mg/L Ag-NPs after exposure of 120 h. The 96-h EC_{50} of Ag-NPs to C. reinhardtii was 32.19 mg/L.

Effects of Ag-NPs on chlorophyll and carotenoid contents of C. reinhardtii

After exposure of Ag-NPs, the contents of chlorophyll a, chlorophyll b, total chlorophylls, and carotenoids in C. reinhardtii cells decreased significantly, and the inhibitory effect tended to increase with increasing Ag-NPs concentrations (Fig. 3a–

Fig. 1 Scanning electron microscope (SEM) image of Ag-NPs (**a**) and particle size distribution of Ag-NPs suspension (**b**)

Fig. 2 Effects of Ag-NPs on the biomass (**a**) and inhibition rate (**b**) of C. reinhardtii

d). The maximum inhibition rate was observed for carotenoids (72.38%) after exposure to Ag-NPs at 50 mg/L for 72 h, followed by chlorophyll a, chlorophyll b, and total chlorophylls (66.48%, 47.80%, 61.46%, respectively). Compared to 0 mg/L, the decreased chlorophyll and carotenoid contents of *C. reinhardtii* under the exposure of Ag-NPs indicated that the photosynthesis was inhibited, which is a potential indicator to show the ecotoxicity effect of Ag-NPs to aquatic organisms.

Cell size, cell viability, and oxidative stress

After 24 h exposure, an obvious decrease ($P < 0.05$) of cell size signal with the increase of Ag-NPs concentration was observed (Fig. 4a). Cell size fluorescence of *C. reinhardtii* in the control group was $5.5 \times 10^4 \pm 72.83$, while it was $4.45 \times 10^4 \pm 1161.07$ under the exposure to 50 mg/L Ag-NPs, which was a decrease of 19%. However, the change trend of cell size fluorescence with different Ag-NPs concentrations was not obvious after 48 h and 72 h of exposures.

The intracellular chlorophyll autofluorescence increased with exposure time (Fig. 4b). And exposure to increased concentration of Ag-NPs can cause a significant decrease ($P < 0.05$) of chlorophyll autofluorescence. Ag-NPs induced cytotoxicity displayed a dose-response relationship. The results were consistent with the results of chlorophyll contents

(Fig. 4a). The reduction of surviving cells in the collected 10,000 cells will also directly lead to a decrease in chlorophyll autofluorescence, indicating that Ag-NPs caused cell apoptosis of *C. reinhardtii*.

PI staining method confirmed the apoptosis of *C. reinhardtii*. As shown in Fig. S1a, it can be clearly seen that 100% heat-damaged cells (positive control) were significantly deviated from normal cells (negative control). Non-viable cells with damaged cell membranes were shifted from the left to the right (Fig. S1a). The treated cells (50 mg/L Ag-NPs, 72 h) significantly deviated from the normal cells (0 mg/L, 24 h) (Fig. S1b) and had a large overlap to the positive control cells (Fig. S1c).

After algae exposure to Ag-NPs, non-viable cells increased compared to the control group (Fig. 4c), especially for higher concentrations of Ag-NPs (10, 30, and 50 mg/L). Exposure of algae to 50 mg/L Ag-NPs for 72 h induced a $27.85 \pm 0.92\%$ increase of non-viable cells for *C. reinhardtii*, compared to the control. These results proved that high concentration of Ag-NPs and prolonged exposure can cause changes in cell membrane permeability, resulting in severe cell damage and even death.

As observed in Fig. 4d, the percentage of affected cells producing oxidative stress increased with increasing exposure concentrations of Ag-NPs. The percentage of algae cells producing oxidative stress was 35.20% at 50 mg/L Ag-NPs after 72 h of exposure. However, no significant differences were observed
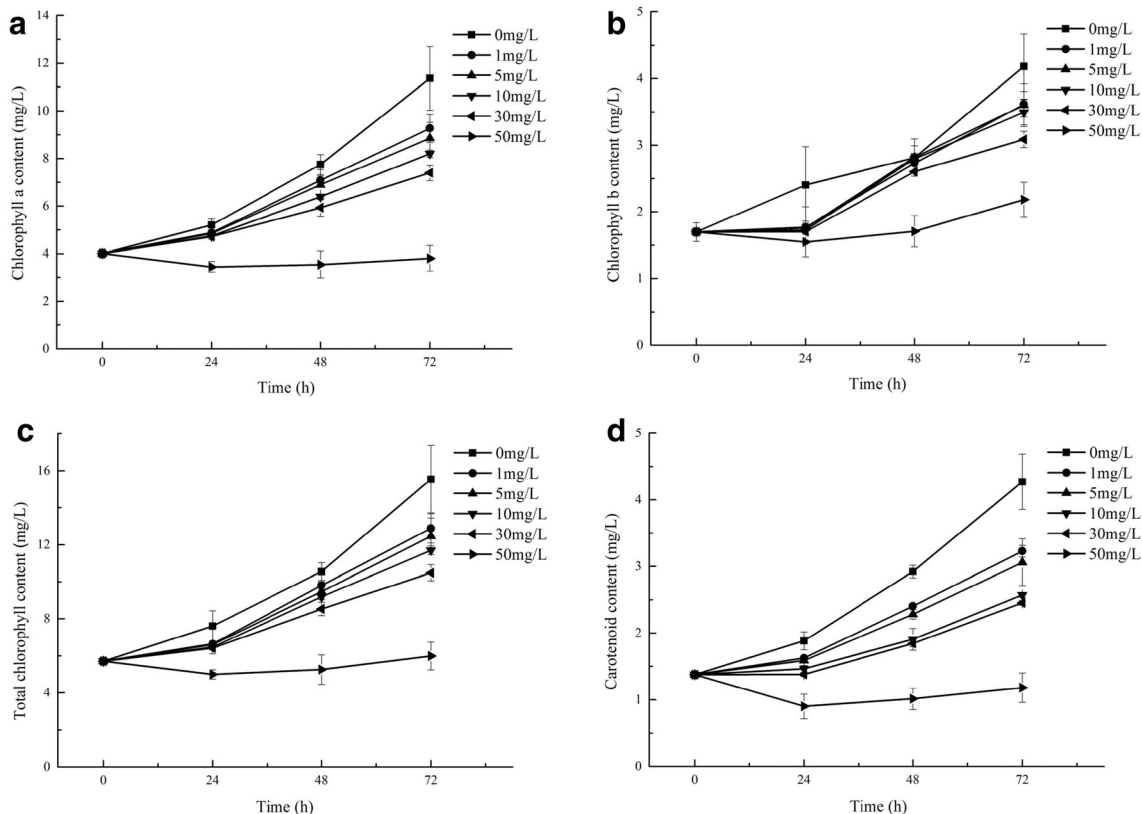
Fig. 3 Effects of Ag-NPs on the contents of chlorophyll a (**a**), chlorophyll b (**b**), total chlorophyll (**c**), and carotenoid (**d**) of *C. reinhardtii*
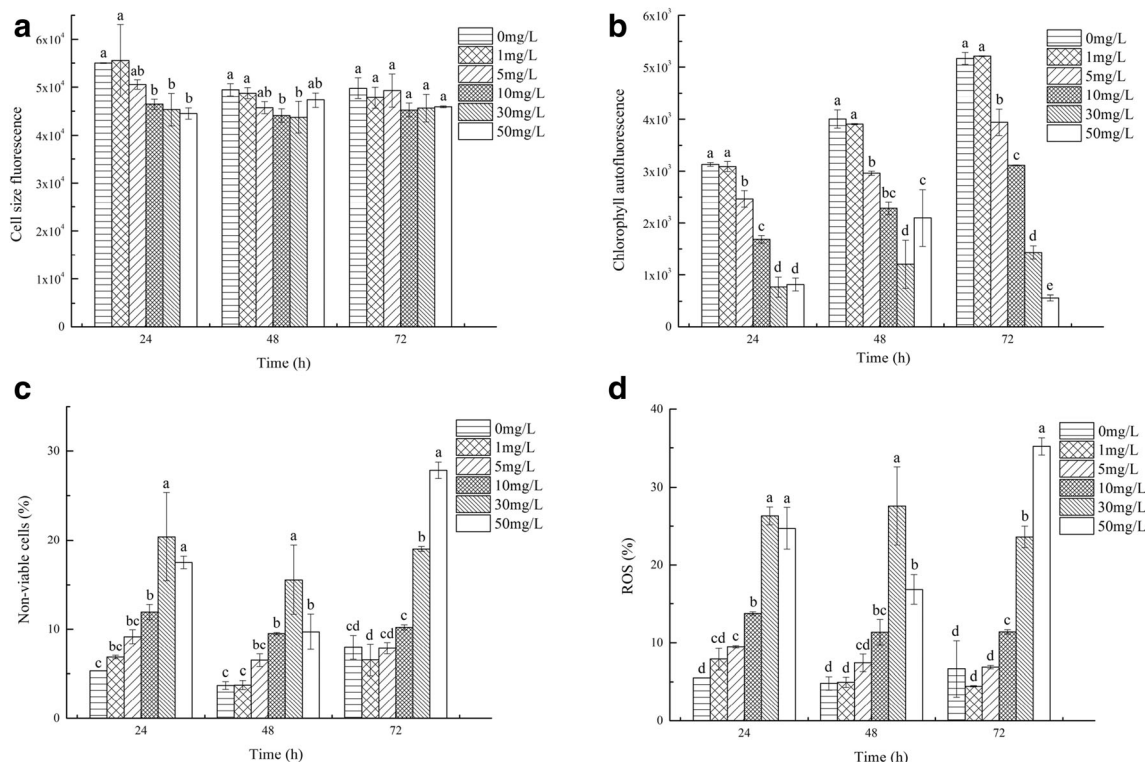
Fig. 4 Effects of Ag-NPs on the cell size fluorescence (**a**), chlorophyll autofluorescence (**b**), non-viable cells (**c**), and percentage of ROS cells produced (**d**) of *C. reinhardtii*. In Fig. C–D, the percentage is relative to the control. Significant difference ($p < 0.05$) between two treatments is presented by different lowercase letters. Error bars represent standard deviation ($n = 3$)

with the increase of the exposure days except 50 mg/L Ag-NPs. The percentage of oxidative stress-producing cells at low exposure concentrations ($< EC_{50}$) even slightly decreased with the increase of exposure time. According to the contour plots of cells producing ROS (Fig. S2a-d), the complexity of cells increased, the number of cells in normal state decreased, and the number of cells under oxidative stress increased. Cells dispersed significantly at 50 mg/L after 72 h, which may be due to excessive toxicity that resulted in death of algal cells.

ROS scavenging enzymes and lipid peroxidation

The changes of SOD and POD activities in cells were caused by oxidative stress. As shown in Fig. 5a, SOD activity increased with increasing Ag-NPs concentrations, but decreased with increasing exposure days. At 72 h exposure, SOD activity of each exposure concentration (1, 5, 10, 30, and 50 mg/L Ag-NPs) was 1.27-, 1.50-, 1.58-, 1.70-, 1.72-fold, respectively, compared to the control. Interestingly, there was almost no difference between the values for 50 mg/L and 30 mg/L Ag-NPs at 72 h, but the differences were significant among the other groups. Compared with the control group, the increase of SOD activity may be due to the excessive production and accumulation of superoxide in *C. reinhardtii* cells.

In the antioxidant defense system, POD is also a key enzyme that converts the generated free radical H_2O_2 into water and oxygen. As observed in Fig. 5b, POD activity fluctuated with Ag-NPs concentrations and exposure time. The activity of POD in algal cells was up to 12.08 U/10^6 cells at 50 mg/L Ag-NPs after 24 h of exposure. The activity of POD at 1 mg/L after 48 h was 1.96 times higher than that of the control group. After 72 h, POD activity reduced to 1.30 U/10^6 cells for the case of 50 mg/L Ag-NPs, while the activities restored to those at 24 h for other Ag-NPs concentrations. These data indicated that Ag-NPs stress could stimulate the activities of antioxidant enzymes and thereby eliminate the damage induced by the environmental stress.

MDA is a molecular indicator of lipid peroxidation, which may damage the structure and function of the cell membrane system (Wang et al. 2008). The degree of lipid peroxidation indicated by the determination of MDA content in *C. reinhardtii* cells in the presence or absence of Ag-NPs. As shown in Fig. 5c, MDA content increased with increasing Ag-NPs concentrations. Compared with the 24 h exposure, MDA levels increased at 48 h for 1, 5, 10, and 30 mg/L Ag-NPs. While for Ag-NPs at 50 mg/L, MDA content was almost constant at different (24– 72 h) exposure durations. Although MDA is cytotoxic, MDA is also present in algae cells without Ag-NPs stress. The MDA content of the control group (0 mg/L, 24 h) increased by 9.49% at 48 h was far less than that under Ag-NPs stress.
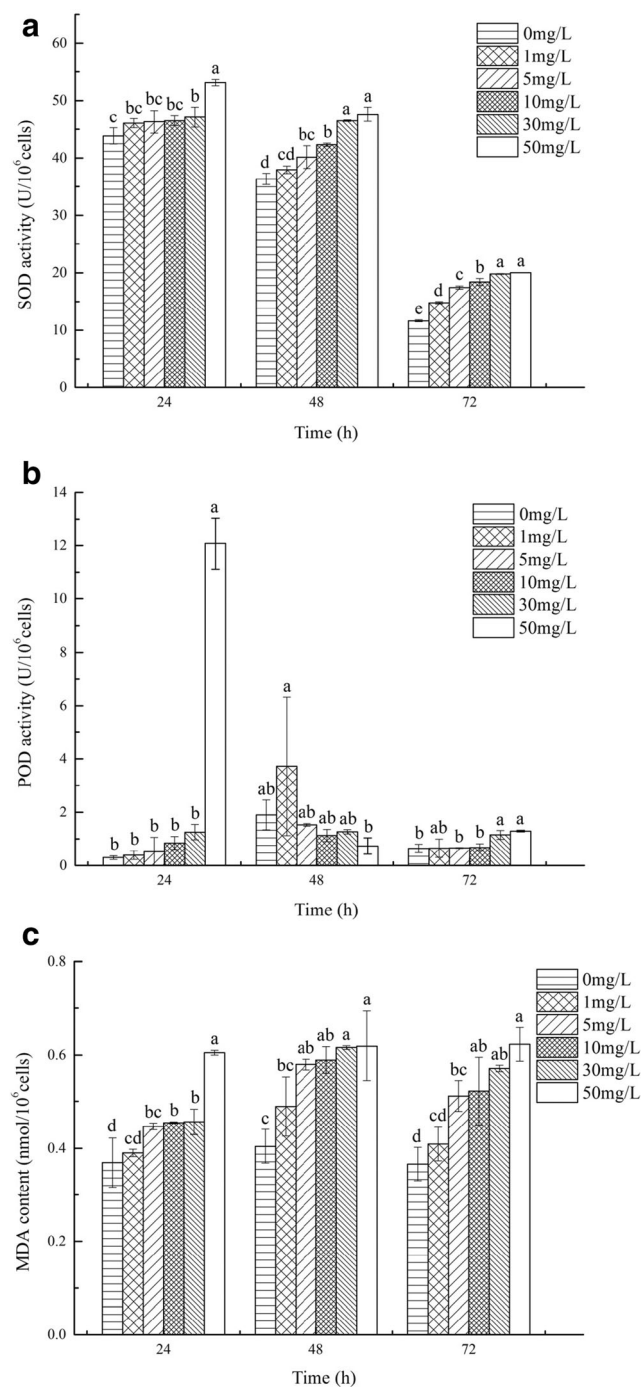
Fig. 5 Effects of Ag-NPs on SOD activity (a), POD activity (b), and MDA content (c) of *C. reinhardtii*. Significant difference ($p < 0.05$) between two treatments is presented by different lowercase letters. Error bars represent standard deviation ($n = 3$)

Effects of Ag-NPs on the ultrastructure of *C. reinhardtii*

The influence of Ag-NPs on the ultrastructure of *C. reinhardtii* was investigated with the TEM measurement in Fig. 6. In the control group, the cell morphology of *C. reinhardtii* was complete, the cell membrane was closely

connected with the cell wall, and there was no plasmolysis (Fig. 6a). And, the internal structure (chloroplast, pyrenoid) of the control cells was intact, the vacuoles were clear and transparent, and no impurities entered (Fig. 6a). After exposure to Ag-NPs at 1 mg/L for 72 h, the cell structure was complete, but Ag-NPs were observed to enter into the wall membrane space, cytoplasm, vacuoles, and other organelles, and no significant plasmolysis was observed (Fig. 6b). After 72 h exposure to 10 mg/L Ag-NPs, the cell structure was destroyed, and a lot of Ag-NPs particles were observed to enter the cells, and the algal cells showed plasmolysis (Fig. 6c).

At 50 mg/L Ag-NPs for 72 h, the protoplasts of some treated cells showed a contracted state, the volume was significantly reduced, the plasma membrane was detached from the cell wall, and the cell wall became thinner (Fig. 6d). In other treatment cells, the cell wall and plasma membrane were completely degraded, the internal structure of the cells were severely damaged, and the cells were damaged and dead (Fig. 6e). These results indicated that Ag-NPs significantly altered the ultrastructure of algal cells, and the excessive concentration of Ag-NPs could even lead to the death of algal cells.

Discussion

Previous studies have found that Ag-NPs are toxic to various plants and animals (Cui et al. 2017; Zhang et al. 2019). The toxicity of Ag-NPs is caused by the internalization of Ag-NPs, the adsorption and shading effect of Ag-NPs, the release of Ag^+ (Li et al. 2014a; Oukarroum et al. 2012; Sendra et al. 2017; Stampoulis et al. 2009). The characterization of Ag-NPs suspension is important because it provides a better understanding of the toxic effects to the organism under test (Lalau et al. 2020). The zeta potential of the Ag-NPs suspension in this experiment indicated that the Ag-NPs surface was negatively charged. Surface charge affect the ability to generate ROS, determine binding sites of receptors, affect dispersion, and aggregation of particles, and thereby affect cytotoxicity (Froehlich 2012). During the experiment, the dissolution of Ag^+ from Ag-NPs was about 0.45%, indicating that the release of Ag^+ was small. Therefore, we could speculate that contribution rate of Ag^+ toxicity was relatively low, and the toxicity of Ag-NPs itself might be the main toxicity. Hu et al. (2018) found that the released Ag^+ contributed to but not key toxicity of Ag-NPs.

Our experimental results show that Ag-NPs significantly inhibit the growth and reproduction of *C. reinhardtii*, and the calculated 96 h-EC$_{50}$ is 32.19 mg/L. Liang et al. (2018) indicated that Ag-NPs showed a significant inhibitory effect on the growth of protonemata in a concentration-dependent manner. The ROS (H_2O_2, •OH and •O_2^-) induced by the redox
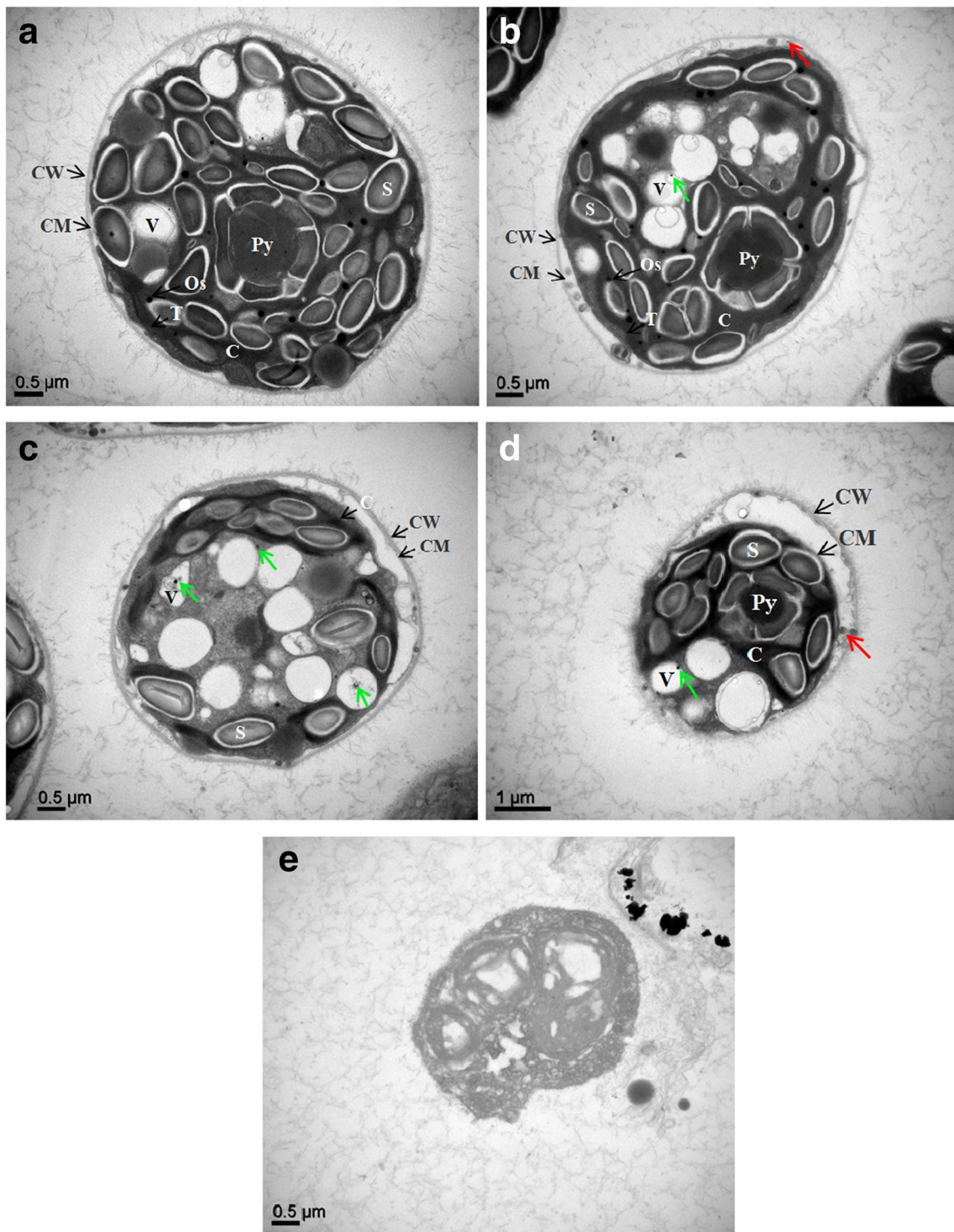
Fig. 6 Transmission electron microscope (TEM) images of *C. reinhardtii* cells in the control (**a**) and after 72 h exposure to 1 mg/L Ag-NPs (**b**), 10 mg/L Ag-NPs (**c**), and 50 mg/L Ag-NPs (**d–e**). The red arrows indicate Ag-NPs entered the cell through endocytosis, and the green arrows indicate Ag-NPs aggregation in vacuole and cytoplasm. CW, cell wall; CM, cell membrane; C, chloroplast; Py, pyrenoid; Os, osmiophilic granules; S, starch grain; T, thylakoids; and V, vacuole

process can destroy almost all types of organic biomolecules (carbohydrates, nucleic acids, lipids, proteins, DNA, and amino acids), so ROS-induced oxidative stress in NPs is considered to be the main mechanism of nanotoxicity (Gong et al.

2019). Our study confirmed that Ag-NPs stress leads to excessive production of ROS by using FCM. Furthermore, our study revealed that, compared to the control, the degree of injury of *C. reinhardtii* exposed to 50 mg/L Ag-NPs for

72 h was in the following order: inhibit growth (78.18%) > carotenoids (72.38%) > chlorophyll a (66.48%) > total chlorophylls (61.46%) > chlorophyll b (47.80%) > cell viability (27.85%, by non-viable cells).

C. reinhardtii growth is inhibited due to its photosynthesis being affected. Previous studies have shown that, under certain stress, the effective quantum yield of PSII is reduced, and photosynthetic pigments are reduced (Liu et al. 2012; Sendra et al. 2018). Our TEM observation revealed that the chloroplast was destroyed, and the channel connecting the pyrenoid and thylakoid region was no longer obvious (10 mg/L and 50 mg/L Ag-NPs). However, after 1 mg/L Ag-NPs exposure, the chloroplast was not damaged, but the photosynthetic pigment content was still reduced, which was probably due to the decrease of thylakoids. Liang et al. (2018) also found that after exposure to Ag-NPs at 2 μg/mL, structural of proton cells was not obviously damaged, but the number of thylakoids in chloroplasts was reduced. Chloroplast damage and reduction of thylakoids lead to the photosynthetic pigments content (chlorophyll a, chlorophyll b, total chlorophylls, and carotenoids) gradually decreased with the increase of Ag-NPs concentration, and the decrease of intracellular chlorophyll autofluorescence was observed with FCM. Other groups have reached similar conclusions by using other creatures (Lalau et al. 2020; Liang et al. 2018).

Heavy metals can cause lipid peroxidation through ROS production (Wahsha et al. 2012). Lipid peroxidation can cause damage to cell membranes, and its main product is MDA (Juganson et al. 2017; Pourrut et al. 2013). In this study, the content of MDA increased with increasing exposure concentration of Ag-NPs, suggesting that lipid peroxidation occurred. Cell membrane permeability and integrity were impaired by excess ROS attack. The internalization of Ag-NPs could be observed as the increase of membrane permeability. The apoptosis of *C. reinhardtii* exposed to high level of Ag-NPs (50 mg/L) occurred, which was characterized by the increase of non-viable cells, decrease of cell size, and phenomenon of plasmolysis. With the increase of exposure durations, the change of MDA content may be due to the decrease of ROS production under low exposure concentration, and the algal cells will restore MDA content to the normal level through their own regulatory ability to reduce cell membrane damage (Li et al. 2014b). However, when the concentration of Ag-NPs reached 50 mg/L, the MDA content was still high because the damage was difficult to recover. The number of non-viable cells at 72 h was almost the same as that at 24 h, which also confirmed the above results.

Plants can use defense mechanisms to resist the harmful effects of ROS (Movafeghi et al. 2017), for instance, the activation of antioxidant enzymes such as SOD and POD. SOD is considered to be the first line of defense in the antioxidant system (Li et al. 2016), which can turn $•O_2^-$ into O_2 or H_2O_2 (Khataee et al. 2012). With the increase of exposure days, the decrease of SOD activity may be due to the decrease of ROS production at low exposure concentrations (Li et al. 2019). With the increase of Ag-NPs concentration, the increase of SOD activity may be due to the direct response of SOD to the production and accumulation of excess superoxide. Previous studies have reached similar conclusions under different creatures and toxic substances stress (Hafsi et al. 2011; Li et al. 2014a). POD is regarded to be the second line of defense in the antioxidant system (Li et al. 2016), which converts H_2O_2 into one of the key enzymes of H_2O and O_2, preventing the formation of •OH (Hazani et al. 2013). When the concentration of Ag-NPs was 50 mg/L for 48 h, the POD activity decreased rapidly, which may be due to the overproduction of ROS, resulting in the change of enzyme molecular structure and damage to the defense system (Van der Oost et al. 2003). The decrease in SOD activity at high exposure concentrations may also be the cause.

Conclusion

In summary, through the systematic experiments of growth inhibition, photosynthesis, oxidative stress, and ultrastructure, we found that Ag-NPs have a significant toxic effect to *C. reinhardtii*. Ag-NPs can damage chloroplasts and inhibit the synthesis of photosynthetic pigments, and thereby inhibit the growth of *C. reinhardtii*. Meanwhile, Ag-NPs will also make the algal cells produce excessive ROS, increase the activities of antioxidant enzymes (SOD and POD), increase the content of MDA, change the cell membrane permeability, destroy the ultrastructure of the cell, and even cause death of algal cells. The degree of injury of Ag-NPs on various biological elements of *C. reinhardtii* is in the following order: inhibit growth > photosynthesis > membrane permeability > ROS production > cell viability. This study is acute toxicity experiments designed to reveal the toxicity mechanism of Ag-NPs. Since the presence of Ag-NPs in the aquatic environment is trace, we will study the chronic toxicity of Ag-NPs to *C. reinhardtii* in the future to lay the foundation for comprehensively evaluating the toxicity of Ag-NPs in the aquatic environment.

Data availability All data generated or analyzed during this study are included in this published article and its supplementary information files.

Compliance with ethical standards

Competing interests The authors declare that they have no competing interests.

References

Boxall, A B A, Chaudhry, Q, Sinclair, C, Jones, A, Aitken, R, Jefferson, B, Watts, C, (2007) Current and future predicted environmental exposure to engineered nanoparticles. CSL

Bruneau A, Turcotte P, Pilote M, Gagné F, Gagnon C (2016) Fate of silver nanoparticles in wastewater and immunotoxic effects on rainbow trout. Aquat Toxicol 174:70–81

Choi Y, Kim H-A, Kim K-W, Lee B-T (2018) Comparative toxicity of silver nanoparticles and silver ions to *Escherichia coli*. J Environ Sci 66:50–60

Cui R, Chae Y, An Y-J (2017) Dimension-dependent toxicity of silver nanomaterials on the cladocerans *Daphnia magna* and *Daphnia galeata*. Chemosphere 185:205–212

Dewez D, Goltsev V, Kalaji HM, Oukarroum A (2018) Inhibitory effects of silver nanoparticles on photosystem II performance in *Lemna gibba* probed by chlorophyll fluorescence. Curr Plant Biol 16:15–21

Echavarri-Bravo V, Paterson L, Aspray TJ, Porter JS, Winson MK, Hartl MGJ (2017) Natural marine bacteria as model organisms for the hazard-assessment of consumer products containing silver nanoparticles. Mar Environ Res 130:293–302

Froehlich E (2012) The role of surface charge in celular uptake and cytotoxicity of medical nanoparticles. Int J Nanomedicine 7:5577–5591

Gong N, Shao K, Che C, Sun Y (2019) Stability of nickel oxide nanoparticles and its influence on toxicity to marine algae *Chlorella vulgaris*. Mar Pollut Bull 149:110532

Hafsi C, Romero-Puertas M, del Río L, Abdelly C, Sandalio L (2011) Antioxidative response of *Hordeum maritimum* L. to potassium deficiency. Acta Physiol Plant 33:193–202

Hazani A, Ibrahim M, Shehata A, El-Gaaly G, Daoud M, Fouad D, Rizwana H, Moubayed N (2013) Ecotoxicity of Ag-nanoparticles on two microalgae, *Chlorella vulgaris* and *Dunaliella tertiolecta*. Arch Biol Sci 65:1447–1457

Hiriart-Baer VP, Lee DY, Campbell PG (2006) Toxicity of silver to two freshwater algae *Chlamydomonas reinhardtii* and *Pseudokirchneriella subcapitata* grown under continuous culture conditions: influence of thiosulphate. Aquat Toxicol 78:136–148

Hoque ME, Khosravi K, Newman K, Metcalfe CD (2012) Detection and characterization of silver nanoparticles in aqueous matrices using asymmetric-flow field flow fractionation with inductively coupled plasma mass spectrometry. J Chromatogr A 1233:109–115

Hu Y, Chen X, Yang K, Lin D (2018) Distinct toxicity of silver nanoparticles and silver nitrate to *Daphnia magna* in M4 medium and surface water. Sci Total Environ 618:838–846

Jagadeesh E, Khan B, Chandran P, Khan SS (2015) Toxic potential of iron oxide, CdS/Ag$_2$S composite, CdS and Ag$_2$S NPs on a fresh water alga *Mougeotia* sp. Colloids Surf B: Biointerfaces 125:284–290

Ji J, Long Z, Lin D (2011) Toxicity of oxide nanoparticles to the green algae *Chlorella* sp. Chem Eng J 170:525–530

Johari SA, Sarkheil M, Tayemeh MB, Veisi S (2018) Influence of salinity on the toxicity of silver nanoparticles (AgNPs) and silver nitrate (AgNO$_3$) in halophilic microalgae, *Dunaliella salina*. Chemosphere 209:156–162

Juganson K, Mortimer M, Ivask A, Pucciarelli S, Miceli C, Orupõld K, Kahru A (2017) Mechanisms of toxic action of silver nanoparticles in the protozoan *Tetrahymena thermophila*: from gene expression to phenotypic events. Environ Pollut 225:481–489

Kachynski A, Kuzmin A, Nyk M, Roy I, Prasad P (2008) Zinc oxide nanocrystals for nonresonant nonlinear optical microscopy in biology and medicine. J Phys Chem C 112:10721–10724

Ke M, Qu Q, Peijnenburg WJGM, Li X, Zhang M, Zhang Z, Lu T, Pan X, Qian H (2018) Phytotoxic effects of silver nanoparticles and silver ions to *Arabidopsis thaliana* as revealed by analysis of molecular responses and of metabolic pathways. Sci Total Environ 644:1070–1079

Khataee A, Movafeghi A, Torbati S, Lisar SY, Zarei M (2012) Phytoremediation potential of duckweed (*Lemna minor* L.) in degradation of C.I. Acid Blue 92: artificial neural network modeling. Ecotoxicol Environ Saf 80:291–298

Lalau CM, Simioni C, Vicentini DS, Ouriques LC, Mohedano RA, Puerari RC, Matias WG (2020) Toxicological effects of AgNPs on duckweed (*Landoltia punctata*). Sci Total Environ 710:136318

Lee D, Fortin C, Campbell PGC (2005) Contrasting effects of chloride on the toxicity of silver to two green algae, *Pseudokirchneriella subcapitata* and *Chlamydomonas reinhardtii*. Aquat Toxicol 75: 127–135

Li M, Zhu L, Lin D (2011) Toxicity of ZnO nanoparticles to *Escherichia coli*: mechanism and the influence of medium components. Environ Sci Technol 45:1977–1983

Li F, Liang Z, Zheng X, Zhao W, Wu M, Wang Z (2014a) Toxicity of nano-TiO$_2$ on algae and the site of reactive oxygen species production. Aquat Toxicol 158:1–13

Li T, Jing YS, Han W (2014b) Growth recovery of microcystis aeruginosa after sub-high temperature stress was relieved. J Appl Ecol 11:3337–3343 (In Chinese)

Li J, Zheng X, Liu K, Sun S, Li X (2016) Effect of tetracycline on the growth and nutrient removal capacity of *Chlamydomonas reinhardtii* in simulated effluent from wastewater treatment plants. Bioresour Technol 218:1163–1169

Li M, Jiang Y, Chuang C-Y, Zhou J, Zhu X, Chen D (2019) Recovery of *Alexandrium tamarense* under chronic exposure of TiO$_2$ nanoparticles and possible mechanisms. Aquat Toxicol 208:98–108

Liang L, Tang H, Deng Z, Liu Y, Chen X (2018) Ag nanoparticles inhibit the growth of the bryophyte, *Physcomitrella patens*. Ecotoxicol Environ Saf 164:739–748

Liu W, Ming Y, Huang Z, Li P (2012) Impacts of florfenicol on marine diatom *Skeletonema costatum* through photosynthesis inhibition and oxidative damages. Plant Physiol Biochem 60:165–170

Lu J, Wang Y, Jin M, Yuan Z, Bond P, Guo J (2020) Both silver ions and silver nanoparticles facilitate the horizontal transfer of plasmid-mediated antibiotic resistance genes. Water Res 169:115229

Manier N, Bado-Nilles A, Delalain P, Aguerre-Chariol O, Pandard P (2013) Ecotoxicity of non-aged and aged CeO$_2$ nanomaterials towards freshwater microalgae. Environ Pollut 180:63–70

Movafeghi A, Khataee A, Abedi M, Tarrahi R, Dadpour M, Vafaei F (2017) Effects of TiO$_2$ nanoparticles on the aquatic plant *Spirodela polyrrhiza*: evaluation of growth parameters, pigment contents and antioxidant enzyme activities. J Environ Sci 64:130–138

Nowicka B, Pluciński B, Kuczyńska P, Kruk J (2016) Physiological characterization of *Chlamydomonas reinhardtii* acclimated to chronic stress induced by Ag, Cd, Cr, Cu and Hg ions. Ecotoxicol Environ Saf 130:133–145

Oukarroum A (2014) Influence of pH on the toxicity of silver nanoparticles in the green alga *Chlamydomonas acidophi*la. Water Air Soil Pollut 225:2038

Oukarroum A, Bras S, Perreault F, Popovic R (2012) Inhibitory effects of silver nanoparticles in two green algae, *Chlorella vulgaris* and *Dunaliella tertiolecta*. Ecotoxicol Environ Saf 78:80–85

Perreault F, Oukarroum A, Melegari SP, Matias WG, Popovic R (2012) Polymer coating of copper oxide nanoparticles increases nanoparticles uptake and toxicity in the green alga *Chlamydomonas reinhardtii*. Chemosphere 87:1388–1394

Pourrut B, Shahid M, Douay F, Dumat C, Pinelli E (2013) Molecular mechanisms involved in lead uptake, toxicity and detoxification in higher plants. Heavy Metal Stress in Plants, pp 121–147

Pröschold T, Harris E, Coleman A (2005) Portrait of a species *Chlamydomonas reinhardtii*. Genetics 170:1601–1610

Sendra M, Yeste MP, Gatica JM, Moreno-Garrido I, Blasco J (2017) Direct and indirect effects of silver nanoparticles on freshwater and marine microalgae (*Chlamydomonas reinhardtii* and *Phaeodactylum tricornutum*). Chemosphere 179:279–289

Sendra M, Blasco J, Araújo CVM (2018) Is the cell wall of marine phytoplankton a protective barrier or a nanoparticle interaction site? Toxicological responses of *Chlorella autotrophica* and *Dunaliella salina* to Ag and CeO_2 nanoparticles. Ecol Indic 95:1053–1067

Stampoulis D, Sinha S, White J (2009) Assay-dependent phytotoxicity of nanoparticles to plants. Environ Sci Technol 43:9473–9479

Suman TY, Radhika Rajasree SR, Kirubagaran R (2015) Evaluation of zinc oxide nanoparticles toxicity on marine algae *Chlorella vulgaris* through flow cytometric, cytotoxicity and oxidative stress analysis. Ecotoxicol Environ Saf 113:23–30

Tran QH, Nguyen VQ, Le A-T (2013) Corrigendum: silver nanoparticles: synthesis, properties, toxicology, applications and perspectives (Adv. Nat. Sci: Nanosci. Nanotechnol. 4 033001). Advances in Natural Sciences: Nanoscience and Nanotechnology

Van der Oost R, Beyer J, Vermeulen NPE (2003) Fish bioaccumulation and biomarkers in environmental risk assessment: a review. Environ Toxicol Pharmacol 13:57–149

Wahsha M, Bini C, Fontana S, Wahsha A, Zilioli D (2012) Toxicity assessment of contaminated soils from a mining area in Northeast Italy by using lipid peroxidation assay. J Geochem Explor 113:112–117

Wang J, Zhang X, Chen Y, Sommerfeld M, Hu Q (2008) Toxicity assessment of manufactured nanomaterials using the unicellular green alga *Chlamydomonas reinhardtii*. Chemosphere 73:1121–1128

Wang Z, Li J, Zhao J, Xing B (2011) Toxicity and internalization of CuO nanoparticles to prokaryotic alga *Microcystis aeruginosa* as affected by dissolved organic matter. Environ Sci Technol 45:6032–6040

Wei D, Unalan H, Han D, Zhang Q, Niu L, Amaratunga G, Ryhänen T (2008) A solid-state dye-sensitized solar cell based on a novel ionic liquid gel and ZnO nanoparticles on a flexible polymer substrate. Nanotechnology 19:222–229

Wiesner M, Lowry G, Alvarez P, Dionysiou D, Biswas P (2006) Assessing the risks of manufactured nanomaterials. Environ Sci Technol 40:4336–4345

Wu Y, Zhou Q, Li H, Liu W, Wang T, Jiang G (2010) Effects of silver nanoparticles on the development and histopathology biomarkers of Japanese medaka (*Oryzias latipes*) using the partial-life test. Aquat Toxicol 100:160–167

Yu Z, Hao R, Zhang L, Zhu Y (2018) Effects of TiO_2, SiO_2, Ag and CdTe/CdS quantum dots nanoparticles on toxicity of cadmium towards *Chlamydomonas reinhardtii*. Ecotoxicol Environ Saf 156:75–86

Zhang C, Hu Z, Li P, Gajaraj S (2016) Governing factors affecting the impacts of silver nanoparticles on wastewater treatment. Sci Total Environ 572:852–873

Zhang CL, Jiang HS, Gu SP, Zhou XH, Lu ZW, Kang XH, Yin L, Huang J (2019) Combination analysis of the physiology and transcriptome provides insights into the mechanism of silver nanoparticles phytotoxicity. Environ Pollut 252:1539–1549